

DOI: <http://dx.doi.org/10.21123/bsj.2021.18.1.0102>

## Synthesis of Bimetallic Au–Pt / TiO<sub>2</sub> Catalysts as an Efficient Catalyst for the Photodegradation of Crystal Violet Dye

*Souad A. Mousa*<sup>1\*</sup>

*Sanaa Tareq*<sup>1</sup>  
*Mohammed. S. Kadhim*<sup>2</sup>

*Eman A. Muhammed*<sup>1</sup>

<sup>1</sup> Department of Chemistry, College of science for women, University of Baghdad, Baghdad, Iraq

<sup>2</sup> Nanotechnology and advance center, University of Technology, Baghdad, Iraq

\*Corresponding author: [souad.mousa17@gmail.com](mailto:souad.mousa17@gmail.com), [sttariq@yahoo.com](mailto:sttariq@yahoo.com), [adnaneman616@gmail.com](mailto:adnaneman616@gmail.com),  
[M.technology85@gmail.com](mailto:M.technology85@gmail.com)

\*ORCID ID: <https://orcid.org/0000-000i-6333-3417>\*

Received 11/11/2019, Accepted 1/4/2020, Published Online First 6/12/2020, Published 1/3/2021



This work is licensed under a [Creative Commons Attribution 4.0 International License](https://creativecommons.org/licenses/by/4.0/).

### Abstract:

Bimetallic Au –Pt catalysts supporting TiO<sub>2</sub> were synthesised using two methods; sol immobilization and impregnation methods. The prepared catalyst underwent a thermal treatment process at 400° C, while the reduction reaction under the same condition was done and the obtained catalysts were identified with transmission electron microscopy (TEM) and energy-dispersive spectroscopy (EDS). It has been found that the prepared catalysts have a dimension around 2.5 nm and the particles have uniform orders leading to high dispersion of platinum molecules. The prepared catalysts have been examined as efficient photocatalysts to degrade the Crystal violet dye under UV-light. The optimum values of Bimetallic Au –Pt catalysts supporting TiO<sub>2</sub> have been found (0.05g of the catalyst prepared in sol immobilization method, 0.07 g of the synthesised in impregnation procedure. The impact of pH on the degradation reaction was tested; it has been found that pH 10 is the best media for the reaction. The effect of temperature has been discussed when various temperatures were used, and the heat of photoreaction E<sub>a</sub> was estimated from the Arrhenius relationship, it has been concluded that the reaction is independent of temperature as the activation energy was very small (E<sub>a</sub>= 22 kJ/ mole). The thermodynamic functions; entropy, enthalpy and the free energy have been figured out. It has been found that the positive values of enthalpy ΔH<sup>#</sup> refer to endothermic reaction, moreover, it has been demonstrated that the photoreaction is an endergonic one according to the calculated values of the free energy of activation. It has been noticed that when temperature increases, it promotes the production of free radicals, but it has been noticed that exceeding the temperature more than the used range causes reducing the percentage of degradation of crystal violet, the reason is due to the limitation conditions of adsorption process at higher temperature on the surface of the catalyst.

**Key words:** Crystal violet, Nanoparticles, Photodegradation, Thermodynamic functions, Titanium dioxide.

### Introduction:

The pollution of natural waters with dyes becomes a serious environmental problem in all countries, while the quantity of dyes in wastewater and release of wastewaters in nature are increasing continuously. Many dyes and their reaction products are very harmful due to the presence of toxicants. Therefore, the dyes must be removed from contaminated effluent water before being released to the environment (1). Crystal violet (CV),

Figure , is a basic dye, which belongs to triphenylmethane dye group that is extensively applied in many industries such as, textiles industry, petroleum waste industry and papers and plastics

industry; it is also employed for biological staining in veterinary medicine. Many studies have been conducted to mineralize the contaminations using various types of methods such as biodegradation (2-6), corrosion process (7), adsorption (8-15) and photodegradation (16-21). One of the most efficient and economical methods is probably photodegradation. Photocatalysis reactions have emerged as a destructive technology employed to decrease the contaminants in waste water (22). Semiconductor metal oxides have been introduced as common photocatalysts. It has been found that, as a result of light irradiation with photons of

energy higher than the band gap of the photocatalyst (about 3.4 eV for TiO<sub>2</sub> anatase), the electrons shift leads to the generation of charged holes in the valance level. It has been reported that the photoreaction can be stopped running by recombining the pair electron-hole or it can reach the particle surface and further generate free radicals such as (<sup>•</sup>OH), which are very efficient oxidizers of organic material and can degrade pollutants (22). Furthermore, it has been pointed out that the downside of using TiO<sub>2</sub> as a photocatalyst is that its band gap lies in the UV area; so only irradiation under ultra-violet rays can generate electron-hole pairs which is considered as the first step in the photoreaction, while ultra-violet rays constitute approximately 5% of the spectrum, which makes a limitation of generating of electron-hole pairs by using TiO<sub>2</sub> as photocatalyst. So, hundreds of studies have been done to withdraw the absorption of TiO<sub>2</sub> to the visible spectrum. Furthermore, the addition of transition metals to the titanium dioxide structures help to pull the absorption to the longer wavelengths (19, 23-27). The aim of this study is to synthesize Bimetallic Au-Pt catalysts / TiO<sub>2</sub> as an efficient catalyst and test it to degrade the crystal violet dye from aqueous solution at different operating conditions.

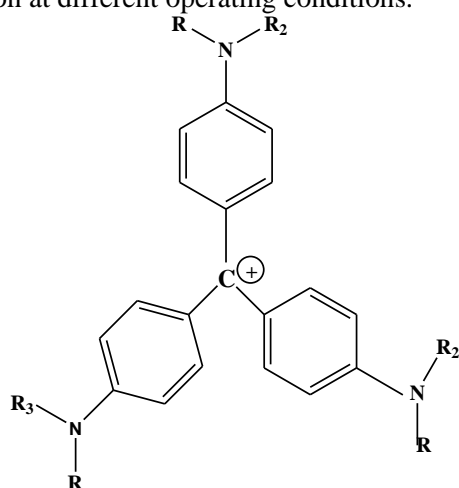


Figure 1. Chemical structure of crystal violet dye

## Materials and Methods

### Chemical

PtCl<sub>2</sub>, TiO<sub>2</sub> (Degussa, P25), HAuCl<sub>4</sub>.3H<sub>2</sub>O, NaBH<sub>4</sub> (>96%), and polyvinyl alcohol (PVA) (molar mass ~ 9,000-10,000 g/mol 80% hydrolyzed) have been taken up from Aldrich. Crystal violet dye has been supplied from HIMEDIA, photocatalyst TiO<sub>2</sub> nanoparticles type anatase 30 nm supplied from US research nanomaterial, Inc., USA with high purity 99.98%, Hydrochloric acid was provided from BDH and

sodium hydroxide was supplied from Riedel-De Haen AG Seelze-Hannover.

### Synthesis of the catalysts

Gold and platinum were loaded on titania, using two techniques; impregnation and immobilization (28).

#### Impregnation technique procedure

A conventional wet impregnation technique was used to create comparisons between Au and Pt individually, and Au/ Pt catalysts, which were besides prepared and supported on TiO<sub>2</sub> (Degussa, P25). The bimetallic Au\ Pt materials were produced using the impregnation technique accompanied by taking an aqueous solution of PtCl<sub>2</sub> (0.01364g/ 10 ml) and HAuCl<sub>4</sub>.3H<sub>2</sub>O (PtCl<sub>2</sub>/ 10 ml) mixed with the scattered TiO<sub>2</sub> (Degussa, P25), in 100 ml water. The mixed substances were stirred at 50 °C until a thick soft mixture was formed. Then the mixed substances were dried at 110 °C for 16 h, lastly the thermal treatment at 400 °C for 3h under rate of heating 20 °C/min was achieved. The photocatalyst synthesized by the impregnation technique has been classified as Au-Pt/ TiO<sub>2</sub> IM. By the same token, a similar procedure was used to prepare the mono molecule of Au and Pt with the desired Au and Pd catalysts ratios.

#### Procedure of sol-immobilization technique

An aqueous solutions of PtCl<sub>2</sub> (Aldrich) and HAuCl<sub>4</sub>.3H<sub>2</sub>O (Sigma Aldrich) have been synthesized at desired concentrations. A solution of Au was supplied to the Pt (II) chloride (Sigma Aldrich) solution under controlled stirring at low rate. Blending was done for 30 minutes, after that, a solution of polyvinyl alcohol at concentration (1 g /20ml) was supplied to the mix Au and Pt and endured with constant blending for 5 minutes. The following step was supplying 0.1 M of primed NaBH<sub>4</sub>, with continuous blending for 30 min, after that the mixture was kept to stirring for other 30 minutes until the colour transfers to the deep hazal.

After 30 min, sol synthesis, suspended substance has been controlled by loading titania. By supplying the sulphuric acid with dynamic stirring, the pH was restricted to be 1-3. The desired Au-Pt amount of the support was determined and controlled in the solution (15). After separating the suspended substance and washing it with water in a couple of hours, the obtained material was dried at 120 °C for approximately 16 hours. A product synthesized using the sol-immobilization technique was marked as Au-Pt/ TiO<sub>2</sub> SI. Mono molecule Au / TiO<sub>2</sub> or Pt / TiO<sub>2</sub> photocatalysts were prepared with different desired ratios by the same procedure.

### Characterization of Catalyst

It has been figured out that X-ray diffraction (XRD) measurements were completed by the powder X-ray diffraction (XRD) by X-ray diffractometer Shimadzu XRD 6000 and diffractometer produced by Nickel-filtered CuK $\alpha$  radiation with the Cu-K $\alpha$  radiation with  $\lambda = 1.5404$  Å at generator current of 30 mA and generator voltage of 40 KeV. The catalysts were analyzed within the range  $2\theta$  from 20°C–80°C. The phases were defined by comparing the empirical samples with the JCPDS powder diffraction file. Field emission scanning electron microscopy (FESEM; JSM-7600F) and transmission electron microscopy (TEM; JEOL JEM-2100) were utilized to identify the properties of results. Energy-dispersive X-ray (EDX) spectroscopy, connected to SEM and TEM was employed in order to identify products structures. Brunauer-Emmett-Teller (ASPA P2020 3Flex version 1.02, that is, it is engaged with nitrogen adsorption–desorption analyser). The hypothesis of BET (physical adsorption of gases molecules on hard surfaces) has been demonstrated, where this theory presents the main principle of the technique of analysis, which measures the material specific surface area (29). The BET equation has usually is written linearly as follows:

$$\frac{P}{n^a (P^o - P)} = \frac{1}{n_m^a C} + \left[ \frac{C-1}{n_m^a C} \right] \frac{P}{P^o} \quad (1)$$

where; V is the volume decreased to the standard condition (STP) of the adsorbed gas per unit mass of catalyst, which represents the adsorbent, P is the particular mass adsorbent, P<sup>o</sup> is the completely moisture pressure at constant temperature, V<sub>m</sub> is the gas volume adsorbed at (STP) per the unit mass of adsorbent when the surface is shielded by a mono molecular layer of adsorbent. C is a constant, associated with the free adsorption energy. However, the previous equation was only applicable at low relative pressures within the range of 0.05 > p/p<sub>o</sub> < 0.3.

### Irradiation system

In this work, the irradiation system (Figure ) consists of Pyrex photoreaction cell 75 ml capacity with a quartz window fitted with a focusing lens to ensure parallel beam of light. The mercury lamp 125 watt is placed 10 cm apart from the photoreaction cell. The cell is supplied with two openings of 0.5 cm in diameter and one of these is used for sampling processes. The magnetic stirrer (wise) from Daihan scientific is used to keep the catalyst aqueous suspension in homogeneous form during the photolysis experiments, and the circulating thermostat (Recirculating chiller) from

Daihan scientific is used to control the reaction temperature. Absorption values were recorded with Visible spectrophotometer model 721 China, all of samples centrifuge using (centrifuge model 800 electric centrifuge), photocatalysts were weighed using Analytic sensitive balance (Sartorius) from Germany.

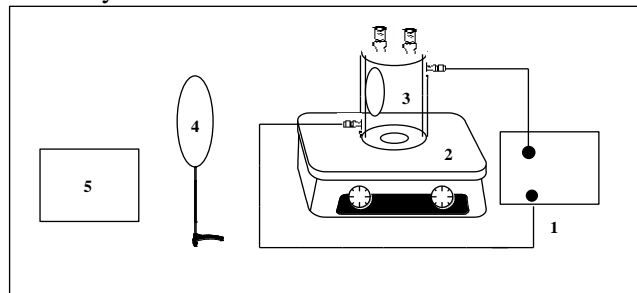


Figure 2 . Irradiation System; 1- Circulator, 2- Magnetic stirrer, 3- Photoreaction Cell, 4-Lens, and 5- UV- Source

### Calibration Curve of CV dye

Stock solution was prepared at concentration 250 ppm used to prepare the solutions employed in the experiments, which was 8 ppm, the standard calibration curve (Fig.3) of crystal violet dye at 585 nm (Fig.4 shows the absorption spectrum of crystal violet) , was used to convert absorbance values of dye to a concentration According to Beer-Lambert law.

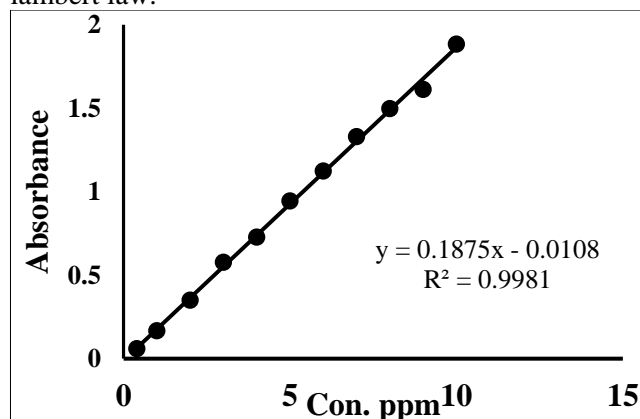


Figure 3. Calibration curve of CV

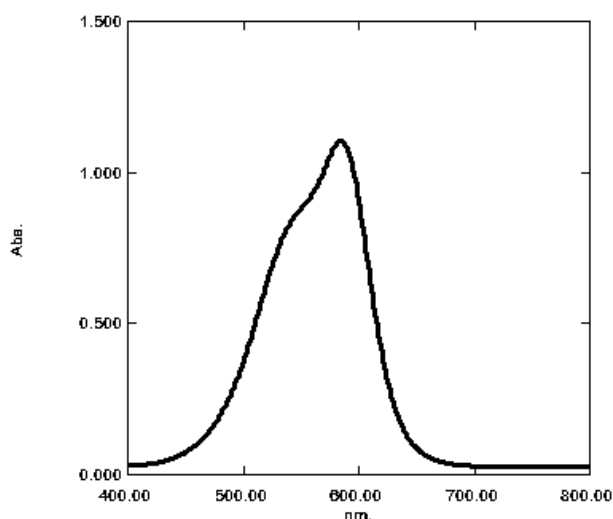


Figure 4. Absorption spectrum of CV dye

### Procedure of Degradation

Before irradiating the dye solutions, the catalysts were added to the crystal violet dye solutions, and then the solutions were stirred during 24hour in dark in order to establish sorption equilibrium of the dye molecules onto surface of the catalysts (18). All of the experiments were carried out in the photoreaction cell using (irradiation system) Figure . Firstly, several amounts of photocatalyst [Au- Pt/ TiO<sub>2</sub>], (0.03-0.09g) were added, then 5ml aqueous solution of mixture from each experiment is taken at various time intervals (1 hour during 6 hours) circulating thermostat is used to control the reaction temperature, while magnetic stirrer is used to mix the mixture, the solutions are irradiated with medium mercury lamp, then photocatalyst is removed from the samples using centrifuge. After that, observing the photolysis process has been controlled by following up the

absorbance of the crystal violet dye at 585 using visible spectrophotometer. A series of experiments is repeated using different pH values (3-12), the pH of the solution adjusting using hydrochloric acid (0.1M) and sodium hydroxide (0.1M) and temperatures (25, 35, 45, and 55°C) to determine the best media and temperature for degradation of dye at optimum values of catalysts.

The photodegradation percentage of Crystal Violet dye is calculated using the following equation. (30)

$$\% D = \frac{C_0 - C_t}{C_0} \times 100 \quad (2)$$

where, % D: The percentage degradation, C<sub>0</sub>: The initial concentration (ppm) at zero time. C<sub>t</sub>: The final concentration (ppm) at any time.

### Results and Discussion

#### Synthesis of Bimetallic Au –Pt catalysts / TiO<sub>2</sub>

#### X-ray diffraction (XRD)

X-ray diffraction (XRD) pattern is used for corresponding the crystallographic temple and purity of the phase of the electrospun product. It can be observed that when the content of the metal is less than 0.5% the diffraction, the size D crystallites of the pattern can be studied by the equation of Debye- Sherrer (31) considering D is the crystal size.

$$Crystallite\ size\ D = \frac{(K \times \lambda)}{(FWHM \times \cos \Phi)} \quad (3)$$

where; K is Sherrer constant, λ is the X-ray wavelength, FWHM is the full peak at the half of maximum, and θ is the Diffraction angle.

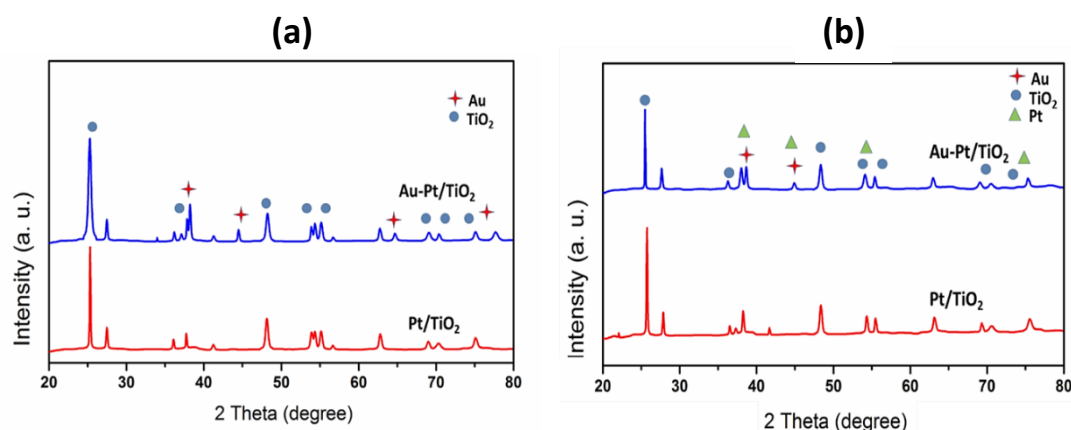


Figure 5. XRD pattern for fresh mono and bimetallic Au-Pd/ TiO<sub>2</sub>, Au-Pd/TiO<sub>2</sub> catalyst synthesized by (a) impregnation and, (b) sol immobilization.

The samples were scanned at 2θ, starting from θ =20- 80°. Figure 5 reveals the similarity of the diffraction peaks profiles in all the products and the fully indexed profiles as the tetragonal anatase

TiO<sub>2</sub> (JCPDS, No.21-1272). All the peaks relating to tetragonal TiO<sub>2</sub> had the sharpest (101) peak. The TiO<sub>2</sub> pure anatase phase was formed at 400 °C, and the rutile anatase phase of TiO<sub>2</sub> is generally known

and has a higher activity than the rutile phase. So, the calcination of the  $\text{TiO}_2$  was done at  $400\text{ }^\circ\text{C}$ . Thermodynamically, the anatase phase has higher stability compared to the rutile phase, and is commonly utilized as a catalyst because oxygen types can smoothly transfer in the anatase phase (32, 33).

Debye- Scherrer formula was utilized to calculate the size of the crystallite from the peaks (101) and (200). The crystallite average size of  $\text{TiO}_2$  was 18 nm approximately for each samples. The XRD patterns (The peaks of Au at  $2\theta = 37.4$  to  $40$  o. was seen clearly to indicate the Au and Pt peaks which are prepared by sol immobilization more clearly than of the calcined sample of 1wt % ( Au-Pd)/  $\text{TiO}_2$ . A slight shift was observed for the Au peaks to the right (increased  $2\theta$  values) which indicated the formation of the Au-Pt alloy as stated in the number of similar studies and the peak sited from the pattern corresponding to the (111) plane (JCPDS 03-065-2870). It has been observed that the Au peaks show the existence of cubic Au (JCPDS, no. 03-065-2870) and/or Pt (JCPDS, No. 40-0802) diffraction peaks for the Au-Pt/ $\text{TiO}_2$  NPs. It has been found that the peaks are comparatively wide; and it was observed as well that the metal of nanoparticles at the surface of  $\text{TiO}_2$  was extremely small and highly discrete or the concentration of the metal was very low for the XRD to be shown. Also, it was not possible to see the sizes of the peaks of metal nanoparticles due to a poor signal exceeding the minimum XRD detection (NPs)(34). There were no notable peaks of Pt associated with the XRD

pattern, it could be because of the minor volume percentage of platinum in  $\text{TiO}_2$ . XRD showed that the films in nature are nanocrystalline with the anatase phase. All the peaks are compatible with tetragonal  $\text{TiO}_2$  at the sharpest (101) peak. By using the Scherrer formula, the mean crystallite size was obtained from (101) and (200) peaks, for Pt sample, there were detected to be 12 nm, while for sample Au there was found to be 18 nm.

For  $\text{TiO}_2$ -Au XPs, the peaks detected at  $37.73^\circ$ ,  $44.03^\circ$ ,  $64.00^\circ$  and  $77.75^\circ$  are a charge of the existence of Au in fcc form with lattice pattern (111), (200), (220) and (311) sequentially (JCPDS file No: 65-2870). Thus, it is not possible to recognize the specific shell metal such as Pt obviously at XRD patterns (35).

#### Transmission electron microscopy

Figure 6 (a) and (b) demonstrate the transmission electron microscopy (CM- 200 Philips (200 kV HT)) of powders gained due to scraping the samples prepared by using different methods. This powder was distributed in ethanol 99.9 %. To carry the powder, Transmission microscopy uses a copper net. TEM images showed the appearance of grains as round and nanocrystal with rate crystallite size of (10.52 nm) for the sample prepared by sol-immobilization and (16.21 nm) for the sample prepared by impregnation method. HRTEM images also showed that there are nanocrystals in the powders and revolve in the films. Figure 6 illustrates the crystalline rate size from XRD and the cereal size from HRTEM and FESEM.

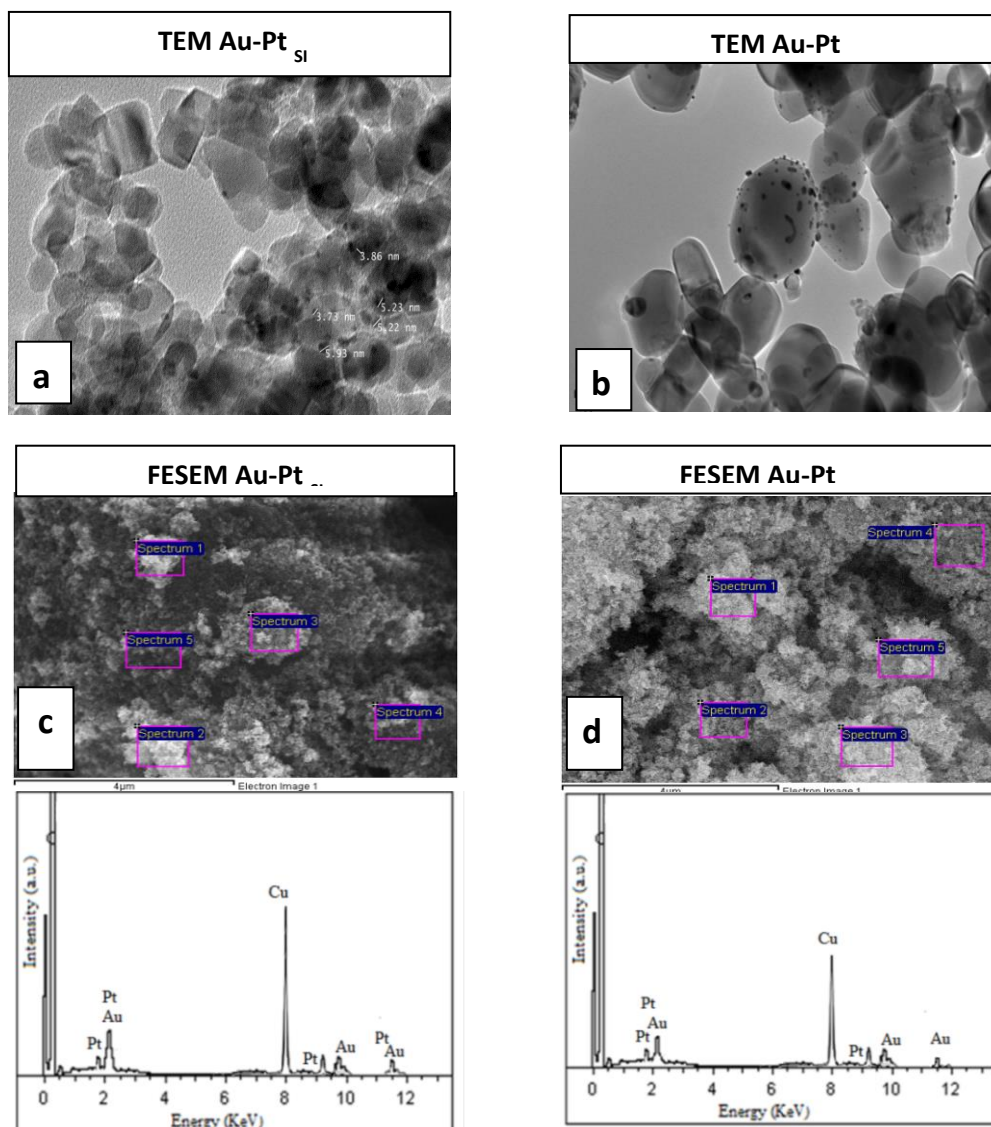


**Figure 6. (a,b) TEM micrographs and the compatible histograms of the particle size distributions for the Au-Pt/TiO<sub>2</sub> specimens synthesized by (a) sol-immobilization, and (b) impregnation, (c-d) (FESEM micrographs and EDX spectrum of (a) 1 wt% (Au-Pt)/ TiO<sub>2</sub>, and (b) 1 wt% (Au-Pt)/ TiO<sub>2</sub>**

Figure 6 (c) and (d) demonstrate that the surface morphology of 1 wt % (Au-Pt) using sol-immobilization and impregnation techniques and calcined at 400 °C had agglomeration correct and this could be due to largely aggregated Au metallic particles. They also show the platinum particles mapping using EDX. The white color signifies the location of platinum. The energy-dispersive X-ray (EDX) spectrum for samples shows further confirmation of the existence of Au and Pt in the nanoparticles(found in the Appendix). A small amount of chloride was detected, which is attributed to the leftover of chlorine compounds from the use of the chloroplatinic acid as the metal precursor, thus it was removed completely from the solution by the washing with (1-2) litter of distilled water. It is thought that higher calcination temperature and longer calcination time could evaporate and purge the chlorine compounds from the catalyst. The

potential platinum particles are high lighted, it can be seen that the surface is porous and rough. It is also not possible to directly observe the Pt nanoparticles without the use of TEM. Despite that, the result from Zhu et al (2013) has shown that catalysts with higher metal dispersion could be obtained with charge enhanced dry impregnation method (36).

#### Surface area analysis of catalyst

The Brunauer- Emmett- Teller (BET) analysis offers an accurate determination of the outer area of a material. Therefore, it provides data on the effectiveness of a catalyst. TiO<sub>2</sub> showed the surface area about 55 m<sup>2</sup> g<sup>-1</sup> when calcination is done at 400 °C for 3 h under air. The complete surface area and the porous structure of the Au-Pt catalyst have been obtained in the circumstance of adsorption-desorption isotherms of nitrogen at 77 K

by using Micro metrics (3 Flex Version 1.02). Each time a pure catalyst of (1.0 – 2.0 g) was inspected. From the estimation, the nitrogen uptake  $P/P_0$  was 1. Table 1 illustrates the reduction in the surface area of 1wt% (Au- Pt)/TiO<sub>2</sub> IM catalyst from 55.0 to 52.0 m<sup>2</sup>/g as a result of feeding Pt and Au metals onto the TiO<sub>2</sub> support. The addition of the metals or the substitution compounds led to the blocking of the pores on the surface of the TiO<sub>2</sub>. For instance, chloride (Cl<sup>-</sup>) could reduce the surface area. However, the BET surface area did not affect due to exposing the 1wt % (Au- Pt)/TiO<sub>2</sub> IM catalyst to several pre-treatments, which indicates the stability of the TiO<sub>2</sub> support.

A reduction in surface area in comparison to the original Titania support could be limited, because of the pore blockage after deposition of platinum nanoparticles at the entrance of the small pores. Mainly, in case of the support itself used as a catalyst, the catalyst has a large surface area and displays the best catalytic activity because the surface area is an active site. However, if a metal is provided on the support, the reaction will take place on the surface of the metal as a result of effectiveness of metal, which is bigger than the support. So the large surface area could then promote the scattering of metal on the surface uniformly. Thus, the metal on the support has a large surface area that could improve catalytic activity.

**Table 1. BET analysis of 5wt% (Au-Pt) with titania- supports prepared using the impregnation and sol-immobilization techniques, calcined in static air at 400 °C for 3 hrs**

| Product   | BET surface area (m <sup>2</sup> /g) |
|---|--------------------------------------|
| TiO <sub>2</sub> (Static air, 400 °C )                  | 55                                   |
| 1% Au/TiO <sub>2</sub> IM                               | 53.5                                 |
| 1wt% (Au- Pt)/TiO <sub>2</sub> IM<br>Static air, 400 °C | 52                                   |
| 1% Au/TiO <sub>2</sub> SI                               | 54.6                                 |
| 1wt% (Au-Pt)/TiO <sub>2</sub> SI                        | 54.2                                 |

Extra analysis related to catalysts synthesized by the sol-immobilization technique showed that TiO<sub>2</sub> continues to have a larger surface area due to its porosity. The 1wt% (Au-Pt) catalysts supported by TiO<sub>2</sub> synthesized using the sol-immobilization technique were found to be comparable to the impregnated catalysts, revealing that the porosity of 1wt% (Au-Pt) enhanced the surface area as shown in Table 1 a which displays that Au-Pt/TiO<sub>2</sub> SI owns a surface area (54 m<sup>2</sup>/g) higher than Au-Pt/TiO<sub>2</sub> IM (52 m<sup>2</sup>/g). Nanoparticles having good ordered penetrable supports provide a great surface area and superior active sites for the catalyst.

It is obvious that the catalysts owning larger surface areas show high catalytic activity (37). The synthesized Au-Pt catalysts display IV isotherm type which is microchannels and show H3 hysteresis curves (29–32) (38-40).

### Photocatalytic reactions

#### Effect of amount of photo catalyst Au-Pt/TiO<sub>2</sub> SI , Au-Pt /TiO<sub>2</sub> IM on crystal violet

The photolysis reaction of crystal violet dye was conducted over a range of the photocatalysts Au- Pt/ TiO<sub>2</sub> (Sol-immobilization method), Au- Pt/ TiO<sub>2</sub> (Impregnation method) amounts (0.03-0.09 g), by using solution of CV at the concentration of 8ppm at temperature 25 °C, the impact of photocatalyst amount on the photodegradation reaction of the dye is shown in

Figure 7 and 8. It can be observed that the rate of photocatalytic reaction of crystal violet is strongly affected by the concentration of the photocatalyst, as the degradation increases with catalyst loading, which means that there are great numbers of energetic positions on the surface of the catalyst as well as more absorbed photons that may enhance the degradation process. But above a certain amount, the efficiency of degradation process decreases, this is because an unfavorable light scattering and depletion in the plane region undergo to light, which resulting a reduction in the penetration into the solution. The optimum dosage of the catalyst must be determined to avoid an excessive amount of catalyst and to ensure the effective photo catalytic process occurred (41). It has been found that the optimum dosage of Au/ Pt/ TiO<sub>2</sub> (prepared by sol-immobilization methods) was 0.05 g where the percentage degradation of crystal violet was (97%). However, the optimum value was 0.07 g of Au/ Pt/ TiO<sub>2</sub> (prepared by impregnation method) and the percentage degradation was (97.6%).

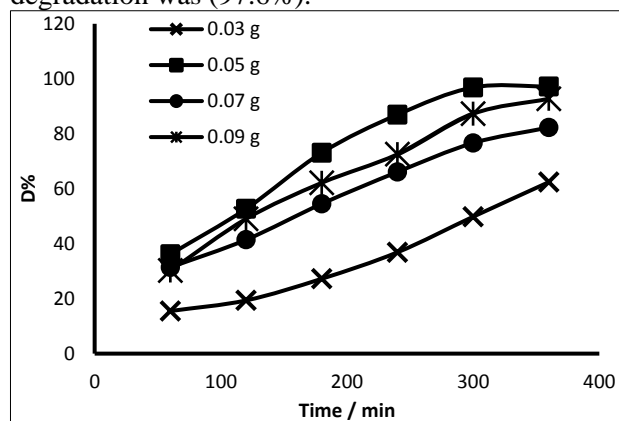


**Figure 7. Percentage degradation of Crystal violet over range of doses of Au- Pt/ TiO<sub>2</sub> SI**

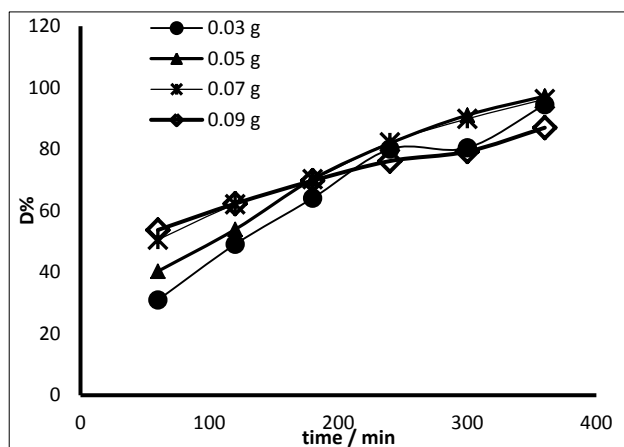


Figure 8. Percentage degradation of Crystal violet over range of doses of Au- Pt/ TiO<sub>2</sub>IM

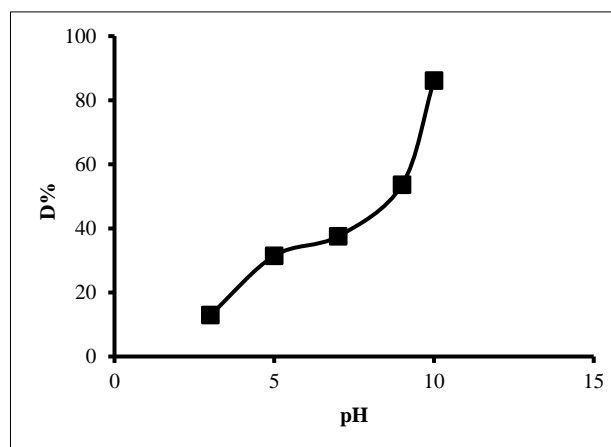


Figure 9. the impact of pH on the degradation of CV dye

### Effect of pH on the photocatalytic reaction

The effect of change in pH values on the photolysis reaction of crystal violet dye at the pH range (3-12) was tested using the catalyst Au- Pt/ TiO<sub>2</sub> (prepared by sol-immobilization) at the optimum dosage (0.05 g), pH of the solutions was adjusted at specific pH by using hydrochloric acid and sodium hydroxide at concentrations 0.1 M, 8ppm was the loading amount of dye at 25 °C. The results of degradation of dye are illustrated in Fig.9. It can be noticed that the photodegradation efficiency of photocatalytic reaction of the dye grows with increasing pH after an hour of irradiation of the solution, and the best pH value for the reaction was at pH 10 as the percentage degradation at pH 10 was 86 % after an hour of irradiation. It is well-known that pH has an impact on the photocatalytic reaction in aqueous media, due to the heterogeneous catalytic reaction occurring on the surface of the catalyst, so that the behavior can be explained depending on the zero point of the catalyst. It has been found that the surface of TiO<sub>2</sub> can be charged or uncharged depending on the acidity or basicity of the media. The zero point charge of the TiO<sub>2</sub> is at 5.9 (42), so it can be predicted at alkaline media that electrostatic attraction can happen between cationic crystal violet dye and negatively charged catalyst surface, which were the controlling forces to support the adhesion of the molecules of the dye and to assist other Photocatalysis reaction. The impact at high pH was studied, at pH 11 the color of dye bleached immediately, when the dye undergoes to irradiation, while at pH 12 the color of crystal violet transfer to colorless without irradiation.

### Effect of temperature on the degradation of crystal violet

Figure 10 shows an influence of changing temperature on the photodegradation reaction of (CV) dye at concentration 8ppm, and illustrates that an increase in reaction temperature results in increasing the degradation of crystal dye at optimum values of catalyst amount and pH of media (0.05 g of Bimetallic Au–Pt catalysts / TiO<sub>2</sub> (sol), pH 10) after irradiation time of 3h. The heat of the photoreaction E<sub>a</sub> was obtained from the Arrhenius equation,

$$\ln k = -\frac{E_a}{R} \left(\frac{1}{T}\right) + \ln A \quad (4)$$

where k is the rate constant of the reaction, R constant of gases, T is temperature in Kelvin and A is the frequency factor. The slope of linear plot of ln k vs. 1/T is equal to -E<sub>a</sub>/R. The thermodynamic parameters have been computed (Table 2) from the mathematic thermodynamic relationships (17):

$$\ln A = \ln(kT/h) + \frac{\Delta S^\#}{R} \quad (5)$$

$$\Delta H^\# = E_a - RT \quad (6)$$

$$\Delta G^\# = \Delta H^\# - T\Delta S^\# \quad (7)$$

Where k is the Boltzmann constant, h is Plank constant, ΔH, ΔS and ΔG are the enthalpy of reaction, entropy and Gibbs energy of the reaction respectively. The obtained activation energy (22.0 kJ/mol) is low, which figured that the photolysis process is temperature unconventional. This behaviour can be explained depending on the photonic process, when the dye solution being irradiated by light, the electron-hole pair is created, which is considered the first step and it is responsible for starting the photoreaction. Furthermore, the photocatalytic reaction does not require heating. It has been recorded that the actual value of heat of reaction of photo reactions E<sub>a</sub> is

very low and nearly to be zero, while the observed value of the heat of reaction  $E_a$  is often very low in the average heating scale (43). The positive values  $\Delta H^\ddagger$  and  $\Delta G^\ddagger$  refer to endothermic reaction and the reaction is non-spontaneous, respectively. It is observed that with increasing temperature, the generating of free radicals increases, but rising the temperature more the used range resulted in decreasing the percentage of degradation of crystal violet. This behaviour can be attributed to that, at higher temperature, the adhesion forces, which attach the substances with the photocatalyst, may be destroyed leading to reduce in degradation efficiency.

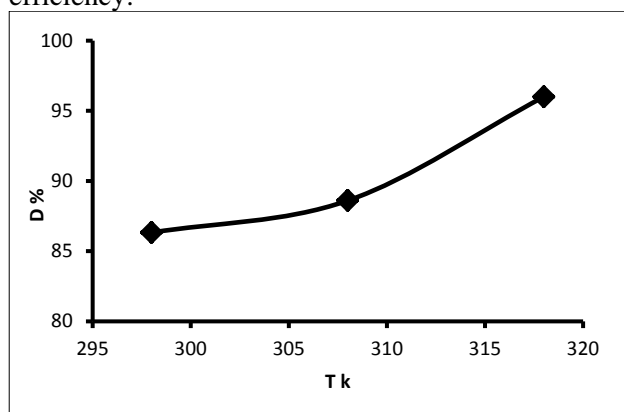


Figure 10. The relation between degradation percentage of crystal violet and temperature (K)

Table 2. Kinetics and thermodynamic parameters values

| T/k | k/h <sup>-1</sup> | $E_a$ /<br>kJ.<br>mol <sup>-1</sup> | $\Delta H^\ddagger$ /kJ.<br>mol <sup>-1</sup> | $\Delta S^\ddagger$ /kJ.<br>mol <sup>-1</sup> | $\Delta G^\ddagger$ /kJ.<br>mol <sup>-1</sup> |
|-----|-------------------|-------------------------------------|---|---|---|
| 298 | 0.0110            |                                     | 19.5  |   | 19.4  |
| 308 | 0.0121            | 22.0                                | 19.4  | 0.25  | 19.3  |
| 318 | 0.0191            |                                     | 19.3  |   | 19.2  |

### Conclusion:

In this study, bimetallic Au –Pt catalysts / TiO<sub>2</sub> have been synthesized utilized two procedures; impregnation and sol immobilization. The new product has been examined by x-ray diffraction (XRD) pattern. Transmission electron microscopy (TEM) has been utilized as well to identify the new prepared catalyst Brunauer-Emmet-Teller (BET) displays surface area of the prepared catalyst. Au-Pt/TiO<sub>2</sub> <sub>SI</sub> and Au-Pt/TiO<sub>2</sub> <sub>IM</sub> catalysts are examined as a photocatalyst in the photodegradation process of crystal violet dye. The operating conditions; quantity of catalysts, pH of media and temperature of the reaction are determined.

### Authors' declaration:

- Conflicts of Interest: None.

- We hereby confirm that all the Figures and Tables in the manuscript are mine ours. Besides, the Figures and images, which are not mine ours, have been given the permission for re-publication attached with the manuscript.
- Ethical Clearance: The project was approved by the local ethical committee in University of Baghdad.

### References:

1. Ciobanu G, Harja M, Diaconu M, Cimpeanu C, Teodorescu R , Bucur D. Crystal violet dye removal from aqueous solution by nanohydroxyapatite. *JFAE*. 2014 Mar; 12(1):499 - 502.
2. Roy DC, Biswas SK, Saha AK, Sikdar B, Rahman M, Roy AK, Prodhan ZH, Tang SS. Biodegradation of Crystal Violet dye by bacteria isolated from textile industry effluents. *PeerJ*. 2018 Jun 21;6:e5015.
3. Mani S, Bharagava RN. Isolation, screening and biochemical characterization of bacteria capable of crystal dye decolorization. *IJAASR*. 2017 Jan; 2 (2):70-75.
4. Selim KA, Abdel-Khalek NA, El-Sayed SM, Abdallah SS. Bioremoval of crystal violet dye from egyptian textile effluent. *IRJET*. 2015 Nov; 2 (8):1038-1043.
5. Ali HM, Shehata SF, Ramadan KM. Microbiol decolorization and degradation of crystal violet dye by *Aspergillus niger*. *Int. J. Environ. Sci. Technol.* 2016 Dec;13(12):2917-2926.
6. Chen CC, Liao HJ, Cheng CY, Yen CY, Chung YC. Biodegradation of crystal violet by *Pseudomonas putida*. *Biotechnol. Lett.* 2007 Jan 6; 29(3):391-396.
7. Oguzie EE. Inhibiting effect of crystal violet dye on Aluminum corrosion in acidic and alkaline media. *J Chem. Eng. Comm.* 2008 Dec; 196(5):591-601.
8. Laskar N, Kumar U. Adsorption of crystal violet from wastewater by modified bambusa tulda. *Journal of civil engineering*. 2018 Aug; 22 (8): 2755-2763.
9. Kusumastuti E, Santosa SJ. Adsorption of crystal violet dye using zeolite synthesized from coal fly ash. *In IOP Conference Series: Materials Science and Engineering 2017 Feb (Vol. 172, No. 1, p. 012028). IOP Publishing.*
10. Harja MA, Ciobanu GA, Favier LI, Bulgariu LA, Rusu LĂ. Adsorption of crystal violet dye onto modified ash. *Bulletin of the Polytechnic Institute from Iași. Chemistry and Chemical Engineering Section*. 2016 Nov;62:27-37.
11. Singh B, Walia BS, Arora R. Parametric and kinetic study for the adsorption of crystal violet dye by using carbonized eucalyptus. *IJCER*. 2018 Sep; 8 (9):1-11.
12. Menkiti MC, Aniagor CO, Agu CM, Ugonabo VI. Effective adsorption of crystal violet dye from an aqueous solution using lignin-rich isolate from elephant grass. *Water Conservation Science and Engineering*. 2018 Jan 6 <https://doi.org/10.1007/s41101-017-0040-4>.
13. Radwan NR, Hagar M, Chaieb K. Adsorption of crystal violet dye on modified bentonites. *Asian J Chem*. 2016 Aug; 28 (8):1643-1647.

14. Salh DM, Aziz BK, Faraidoon K. Adsorption of crystal violet on walnut shell from aqueous solution. *IJBAS*. 2015 Aug; 15(4):4-8.
15. Dandge R, Ubale M, Rathod S. Adsorption of crystal violet dye from aqueous solution onto the surface of green peas shell. *JOAC*. 2016; 5(4):792-801.
16. Papp Z. Unmodified and gold-modified semiconductor catalysts for solar light assisted photodegradation of crystal violet. *Studia Ubb Chemia LX II*. 2017; 1:195-202.
17. Suhail FS, Mashkour MS, Saeb D. The study on photodegradation of crystal violet by polarographic technique. *IJBAS*. 2015; 15 (3):12-19.
18. Weyermann C, Kirsch D, Vera CC, Spengler B. Evaluation of the photodegradation of crystal violet upon light exposure by mass spectrometric and spectroscopic methods. *J. Forensic Sci.* 2009; 54 (2): 339-345.
19. Soliman AM, Elsuccary SA, Ali IM, Ayesh AI. Photocatalytic activity of transition metal ions-loaded activated carbon: Degradation of crystal violet dye under solar radiation. *J WATER PROCESS ENG*. 2017 June; 17, 245-255.
20. George P, Dhabarde N, Chowdhury P. Photo-decolorization of crystal violet using MIL-53(Fe). Conference Paper (68th annual session of indian institute of chemical engineers. 27-30 December 2015. Guwahati, India.
21. Habib MA, Muslim M, Shahadat MT, Islam MN, Ismail IM, Islam TS, et al. Photocatalytic decolorization of crystal violet in aqueous nano-ZnO suspension under visible light irradiation. *JNSC*. 2013; 3: 70.
22. Oller I, Malato S, Sa´nchez-Pe´rez JA. Combination of advanced oxidation processes and biological treatments for wastewater decontamination—A review. *Sci. Total Environ*. 2011; 409(20): 4141–4166.
23. Magalhães P, Andrade L, Nunes OC, Mendes A. Titanium dioxide photocatalysis: fundamentals and application on photoinactivation. *Rev. Adv. Mater. Sci.* 2017; 51(2): 91-129.
24. Primo A, Corma A, Garcia H. Titania supported gold nanoparticles as photocatalyst. *Phys. Chem. Chem. Phys.* 2011; 13(3): 886–910.
25. Paola AD, Ikeda S, Marci G, Ohtani B, Palmisano L. Transition metal doped TiO<sub>2</sub>: physical properties and photocatalytic behavior. *Int J Photoenergy*. 2001; 3(4):171-176.
26. Khairy M, Zakaria W. Effect of metal-doping of TiO<sub>2</sub> nanoparticles on their photocatalytic activities toward removal of organic dyes. *Egyptian Journal of Petroleum*. 2014; 23(4):419–426.
27. Tsang CA, Li K, Zeng Y, Zhao W, Zhang T, Zhan Y, et al. Titanium oxide based photocatalytic materials development and their role of in the air pollutants degradation; overview and forecast. *Envir Int*. 2019 April; 125: 200-228.
28. Tareq S, Taufiq Yap YH, Saleh TA, Abdullah AH. Synthesis of bimetallic gold-palladium loaded on carbon as an efficient catalysts for the oxidation of benzyl alcohol into benzaldehyde. *J Mol Liquids*. 2018; 271:885-891.
29. Brunauer S, Emmett PH, Teller E. Adsorption of gases in multimolecular layers. *J. Am. Chem. Soc.* 1938; 2 (60):309-319.
30. Kumar BN, Anjaneyulu Y, Himabindu V. Comparative studies of degradation of dye intermediate (H-acid) using TiO<sub>2</sub>/UV/H<sub>2</sub>O<sub>2</sub> and photo-Fenton process. *J Chem. Pharm. Res.* 2011; 3(2):718-731.
31. Aldbea FW, Ibrahim NB, Abdullah MH, Shaiboub RE. Structural and magnetic properties of Tb<sub>x</sub>Y<sub>32-x</sub>Fe<sub>5</sub>O<sub>12</sub> (0 ≤ x ≤ 0.8) thin film prepared via sol-gel method. *Journal of sol-gel sci techn.* 2012; 62.
32. Cheng H, Selloni A. Energetics and diffusion of intrinsic surface and subsurface defects on anatase TiO<sub>2</sub> (101). *J. Chem. Phys.* 2009; 131(5).
33. Buchalska M, Kobielski M, Matuszek A, Pacia M, Wojtyła S, Macyk W. On oxygen activation at rutile- and anatase-TiO<sub>2</sub>, *JACS Catalysis*. 2015; 5(12):7424-7431.
34. Reszczynska J, Esteban DA, Gazda M, Zaleska A. Pr-doped TiO<sub>2</sub>. The effect of metal content on photocatalytic activity. *Physicochem Probl MI*. 2014; 50: 515-524.
35. Haijuan L, Haoxi W, Yujuan Z, Xiaolong X, Yongdong J. Synthesis of monodisperse plasmonic Au core-Pt shell concave nanocubes with superior catalytic and electrocatalytic activity. *ACS catal*. 2013; 3: 2045-2051.
36. Zhu X, Cho H, Pasupong M, Regalbutto JR. Charge-enhanced dry impregnation: a simple way to improve the preparation of supported metal catalysts. *ACS Catal*. 2013; 3(4): 625-630.
37. Lopez N, Janssens TV, Clausen BS, Xu Y, Mavrikakis M, Bligaard T, et al. On the origin of the catalytic activity of gold nanoparticles for low-temperature CO oxidation, *J Catal*. 2004; 223(1): 232-235.
38. Mohamed E. Characterization of porous solids and powders; surface area, pore size and density by S.Lowell (Quantachrome instruments, Boynton Beach). *JACS*. 10 Sept. 2005; 127(40)14117.
39. Lowell S, Shields JE, Thomas MA, Thommes M. Characterization of porous solids and powders: surface area, pore size and density. *Springer Science and Business Media*; 2012. 16.
40. Landers J, Gor GY, Neimark AV. Density functional theory methods for characterization of porous materials. *Colloids and Surfaces A: Physicochem and Engin Aspects*. 2013; 437: 3-32.
41. Gaya UI, Abdullah AH. Heterogeneous photocatalytic degradation of organic contaminants over titanium dioxide: A review of fundamentals, progress and problems. *J Photochem Photobio C: Photochem Rev*. 2008; 9:1–12.
42. Komulski M. The significance of the difference in the point zero charge between rutile and anatase. *Adv. Colloids Interface*. 2002; 99: 255-264.
43. Gajbhiye SB. Photocatalytic degradation study of methylene blue solutions and its application to dye

## تصنيع العوامل المساعدة ذهب- بلاتين / ثاني اوكسيد التيتانيوم كعوامل نشطة في عملية التجزئة الضوئية لصبغة الكرسنال البنفسجية

محمد سلمان كاظم<sup>2</sup>ايمان عدنان محمد<sup>1</sup>سناء طارق سرحان<sup>1</sup>سعاد عبد موسى<sup>1</sup>

<sup>1</sup> قسم الكيمياء، كلية العلوم للبنات، جامعة بغداد، بغداد، العراق  
<sup>2</sup> مركز النانوتكنولوجي، الجامعة التكنولوجية، بغداد، العراق

### الخلاصة:

العامل المساعد ذهب- بلاتين/ ثاني اوكسيد التيتانيوم تم تحضيره بطريقتين هما طريقة تراكم الجل وطريقة النقع. ان العوامل المساعدة المحضرة تم ترسيبها تحت درجة 400 درجة مئوية واختزلت تحت ظروف متشابهة وتم تشخيصها باستخدام عدد من التقنيات ومنها مطيافية الالكتران الانتقالية ومطيافية تشتت الطاقة. ان استخدام مواد البريكاسا العنقودية ثنائية المعدن ولدت عوامل مساعدة غير منتظمة الشكل وقطر الدقيقة المتكونة صغير جدا تصل الى 2.5 نانومتر. تم اختبار العوامل المساعدة المحضرة كعوامل مساعدة ضوئية في تفاعلات التحلل الضوئي لصبغة الكرسنال البنفسجية وتم تحديد كمية العامل المساعد المثلى المستخدمة في تفاعلات التحلل الضوئي وكانت 0.05 غم من العامل المساعد المحضر بطريقة التراكم الجل في حين كانت 0.07 غم من العامل المساعد المحضر بطريقة النقع. كما تم دراسة تأثير الدالة الحامضية على وسط التفاعل ووجد ان دالة الحامضية 10 هي افضل وسط لتفاعلات التحلل الضوئي لصبغة الكرسنال البنفسجية. كما تم دراسة تأثير درجة الحرارة على عملية التجزئة الضوئية للصبغة ومناقشة النتائج المستحصلة ففي حالة زيادة درجة الحرارة وباستخدام معادلة ارينيوس تم الحصول على طاقة التنشيط للتفاعل وكانت قيمتها قليلة جدا (طاقة التنشيط = 22 كيلو جول / مول) مما يؤكد عدم اعتمادية التفاعل على درجة الحرارة. ومن قيم ثابت معدل السرعة وطاقة التنشيط المستحصلة من تطبيق معادلة ارينيوس تم حساب قيم الدوال الثرموداينميكية (الانثالي ، الانتروبي والطاقة الحرة لكيبس) وقد بينت النتائج ان التفاعل ماص للحرارة حيث ان قيم الانثالي كانت موجبة وان قيم الطاقة الحرة لكيبس الموجبة تشير الى ان التفاعل غير تلقائي. الا ان الاستمرار في زيادة درجة الحرارة يؤدي الى التقليل من التحلل الضوئي لصبغة الكرسنال البنفسجية وهذا يعزو الى تأثير درجة الحرارة على عملية امتزاز الصبغة على سطح العامل المساعد حيث ان ارتفاع درجات الحرارة يحدد عملية الامتزاز .

**الكلمات المفتاحية:** صبغة الكرسنال البنفسجية، الدقائق النانوية، التجزئة الضوئية، الدوال الثرموداينميكية، ثاني اوكسيد التيتانيوم .